ASEE AMERICAN SOCIETY FOR ENGINEERING EDUCATION

Paper ID #35092

An Improved Magnetically Bistable Piezoelectric Energy Harvester

Carolyn Fulton, Schreiner University

Ms. Fulton is currently an undergraduate research student of the Mathematics Department at Schreiner University in Kerrville, Texas. Her research interests include applied mathematics in the fields of biology, physics, and engineering.

Dr. Brian P. Bernard, Schreiner University

Following receipt of his BSE in Mechanical Engineering from Tulane University, Brian Bernard served 7 years as a nuclear power officer in the submarine force of the US Navy, during which time he also taught 2 years in the Naval Science Dept at the University of Pennsylvania. Brian received his PhD in Mechanical Engineering from Duke University, and is currently an Associate Professor of Engineering at Schreiner University in Kerrville, TX. His technical research is in the field of non-linear dynamics and his educational research is in expanding engineering opportunities on liberal arts campuses.

Prof. Brian P. Mann, Duke University

Dr. Brian Mann is an endowed Professor of Mechanical Engineering at Duke University. He received his BS degree in 1996 from the University of Missouri prior to accepting a position with McDonnell Douglas Corporation. Three years later, he accepted a position in the automotive industry with DaimlerChrysler and earned a M.S. degree at Washington University in St. Louis. Upon deciding to return for his D.Sc. degree, he was awarded the National Defense Science and Engineering Graduate Fellowship. He completed his D.Sc. degree at Washington University in 2003 and has held faculty positions at the University of Florida, University of Missouri, and Duke University. He has received several prestigious early career awards, such as the NSF CAREER Award from the National Science Foundation, the 2007 SAE Ralph Teetor Educator Award, and the Office of Naval Research Young Investigator Award. His present research interests include innovative applications of nonlinear systems theory, energy harvesting, and investigating the stabilizing/destabilizing influence of time delays in systems.

An Improved Magnetically Bistable Piezoelectric Energy Harvester

Carolyn Fulton, Brian P. Bernard
Department of Mathematics, Engineering and Physics
Schreiner University

Brian P. Mann
Department of Mechanical Engineering and Material Science
Duke University

Abstract

By modeling a piezoelectric cantilever beam system in which mechanical bistability emerges from repulsion between a stationary magnet and magnetic tip mass, the size of the basin of attraction for interwell oscillations is increased, so that the higher-energy solutions to the system may be more readily acquired than in previously studied systems. The primary drawback of linear energy harvesters is their very narrow frequency range. Non-linear harvesters provide wider operating frequency regions, but can have coexisting solutions, with the desirable high energy solution usually the more difficult to obtain. Existing work on bistable piezoelectric harvesting systems consider dipole interactions between the magnetic tip mass and an external magnet that is also oscillating at the experimental frequency. This paper demonstrates increased energy generation in transitions between the potential wells of the system through replacing the oscillating independent magnet with a stationary one. Optimizing the system to produce frequent well escapes induced by minimal disturbances from dipole interactions, frequency alterations, or changes in excitation amplitude will aide in achieving the high amplitude solutions of the system. Analytical evaluations of the energy in this system along with simulations of the behavior of the cantilever beam are performed for proof of concept that may be utilized in producing these high amplitude solutions in future experiments.

Introduction

Recent decades have seen an increase in small electrical devices deployed for monitoring and other similar uses. When in cities or accessible areas, even if permanent connection to the electrical grid isn't possible, battery power is a feasible alternative. However in remote locations, periodic battery replacement would be overly burdensome and so renewable resources are required. Vibration energy harvesting can be one such method for renewable energy in suitable environments. Common examples of mechanisms utilized for this intent includes variable capacitance, electromagnetic induction, and piezoelectricity [1].

Proceedings of the 2021 ASEE Gulf-Southwest Annual Conference
Baylor University, Waco, TX

In the study of piezoelectric energy harvesters, the cantilever beam is a common model used [2, 3], and a tuned linear beam can provide higher power output than alternatives, but comes with drawbacks, most significantly, a very narrow frequency range. If the harvester is not perfectly tuned, or if environmental frequency varies, the linear harvester will struggle. Arrays of multiple linear harvesters have been designed to allow a wider operating frequency band without losing maximum power output, but these come with significantly higher cost [4,5]. Nonlinear harvester designs have been proposed to overcome these hurdles. Both softening and hardening style nonlinear beam models have shown to provide a much wider usable frequency range than a single linear oscillator, but with lower maximum power output. The use of coupled beams [6] or dynamic magnifiers [7] have shown improved peak power performance, but another drawback of softening and hardening oscillators is that they have multiple stable equilibria and the high energy equilibrium is the most difficult to obtain experimentally.

Bistable non-linear energy harvesters are an attempt to obtain the wide frequency band benefit of softening and hardening harvesters, but with an easier to obtain high energy solution. Two common designs for bistable harvesters are a buckling beam [8, 9] with pinned attachments at each end but separation distance between the endpoints slightly shorter than beam length, and the cantilever beam with an external force preventing the tip from resting in the neutral center position [10, 11]. In one previous study, the cantilever beam bistability was induced with a magnetic tip mass and an excited external magnet that moved along with the beam's fixed end [12]. This design is still heavily reliant on tuning, in particular in controlling the distance between the tip mass and external magnet, which if too close, will result in only low amplitude intrawell oscillations when external excitation amplitude is low. In this study, we will consider an alternative model in which the external magnet is fixed or is has passively controlled separation distance while still remaining on the absolute centerline. This has the immediate benefit of making high energy interwell oscillation easier to obtain, which strengthens the advantage of the bistable design over softening and hardening alternatives.

This system will be shown to also exhibit a third type of behavior that is not purely intrawell or interwell oscillation, but instead a combination of both. Two common ways of inducing frequency up-conversion are impact [13, 14] and snap-through. The terms twinkling [15, 16] and plucked [17, 18] have been used to describe snap-through induced frequency up-conversion, where low amplitude excitation results in higher amplitude vibration in the system after forcing an oscillator to change from one equilibrium to another. Beneficial frequency up-conversion has also been observed in previous cantilever beam experiments with stochastic excitation [19]. From an energy harvesting perspective, this increase in frequency provides a significant increase in relative velocity of the tip mass, which is positively correlated with energy output.

The following sections will start by establishing the mathematical model for the proposed design. We will then provide numerical simulations demonstrating behavior in several environmental conditions. Lastly, a comparison between a stationary external magnet and two different passively controlled models are provided to demonstrate their relative advantages against each other.

System Description

The primary structure analyzed in this paper is a fixed-free cantilever beam with magnetic tip mass as seen in Fig. (1). If we assume that the magnetic force will have a much larger impact on the beam's displacement than the torque exerted on the magnetic tip mass due to their misaligned angles, then the

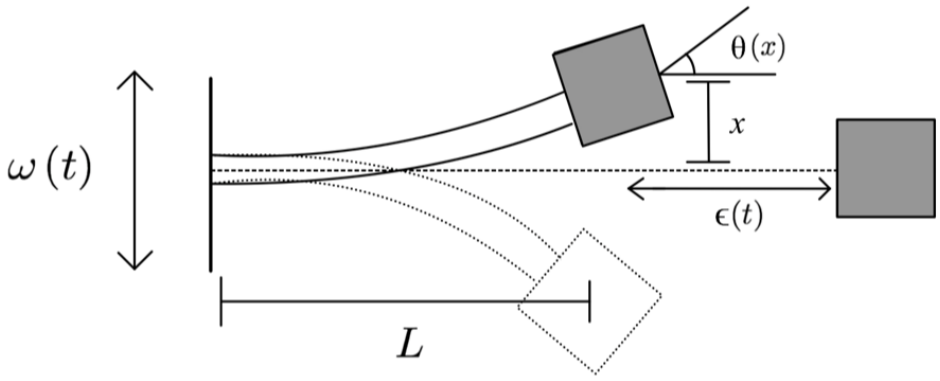

Fig. 1: An illustration of the modeled harvester setup of a stationary magnet separated by distance $\epsilon(t)$ from an oscillating cantilever beam of length L with an attached repulsive magnetic tip mass displaced to a position of x and deflected at an angle of θ. Tip mass and stationary magnets are identical in size and composition.

angle theta can be represented as a function of displacement as follows

$$\theta(x) = \frac{3(x-w)}{2L}, \tag{1}$$

where $(x-w)$ is the difference between the fixed and free ends of the cantilever beam and L the length of the beam.

The external magnet remains in an unrotating position, but able to move linearly left/right to decrease or increase respectively the separation distance between itself and the tip mass magnet. The fixed end of the beam is excited by single frequency excitation, with position represented by

$$w(t) = A \sin \Omega t, \tag{2}$$

where A represents the excitation amplitude in meters and t the time in seconds.

Separation distance is then a function of the absolute value of excitation according to

$$\epsilon_1(t) = \epsilon_0 - BA(t), \tag{3}$$

or

$$\epsilon_2(t) = \epsilon_0 - B|w(t)|, \tag{4}$$

where a coefficient of $B = 0$ would be the case of a stationary magnet at distance ϵ_0 from the tip mass, and $B = 1$ would have the external magnet passively move closer to the beam as excitation increases. However, whereas Eq. 3 provides a stationary external magnet with position dependent on excitation amplitude (and thus would be stationary if amplitude is constant), Eq. 4 would result in the external magnet oscillating such that the magnet would move further away from the beam when excitation approaches the central zero position, then return closer as excitation gets further from the zero position. As

Table 1: Physical parameters of the system that were held constant throughout the analysis unless otherwise noted. System section refers to the placement of the beam with tip mass attached before simulation.

Beam

Parameter	Value	Symbol
Length	0.1 m	L
Height	0.002 m	–
Width	0.006 m	–
Moment of Inertia	$4.0 \cdot 10^{-12}$ m^4	I
Young's Modulus	$3.0 \cdot 10^9\ Pa$	E

Magnet

Parameter	Value	Symbol
Mass	0.0128 kg	m
Volume	$1.6088 \cdot 10^{-6}$ m^3	$V1, V2$
Permeability of Free Space	$4\pi \cdot 10^{-7}$ m $*$ kg	μ_0
Magnetization	$1.05 \cdot 10^6$ A/m	M

System

Parameter	Value	Symbol
Initial Position	0.020165 m	x_i
Initial Gap	0.03 m	ε_0

future sections will demonstrate, each method can provide advantages and disadvantages depending on whether high amplitude beam displacement is preferred, or if intrawell frequency up-conversion is preferred behavior. Either external magnet model provides a method of tuning to avoid the low frequency, low amplitude oscillations possible when the tip mass is stuck in a single potential well, by allowing the potential curve to change based on the excitation amplitude, in particular to allow potential well escape to be more forgiving and easier to obtain when excitation amplitude is low.

Mathematical Model

The piezoelectric energy harvester under investigation has induced mechanical nonlinearity and in many physical configurations, static bistability, by means of repelling dipoles on the tip mass and external magnets. Figure (2) shows the potential energy curve for varying tip mass positions for the case where the beam's fixed end is at the zero position (aligned with the external magnet), the asymmetric nature of the curve when the beam's fixed end is excited slightly to one side of the external magnet, and also shows that when excitation amplitude is high, system constants can be setup that will force the tip mass to cross the external magnet with only a single equilibrium existing when the beam's fixed end is shifted very far from the centerline. The potential energy in the system is calculated as a sum of the beam's strain potential energy and potential energy between the two dipoles. With the beam modeled as a linear Euler-Bernoulli beam, the potential energy is represented by

$$U_s = \frac{3EI}{2L^3}(x-w)^2, \tag{5}$$

where E is Young's Modulus, I the Area Moment of Inertia, L the length of the beam. Since x is the absolute displacement of the tip mass and w the displacement of the beam's fixed end, the quantity

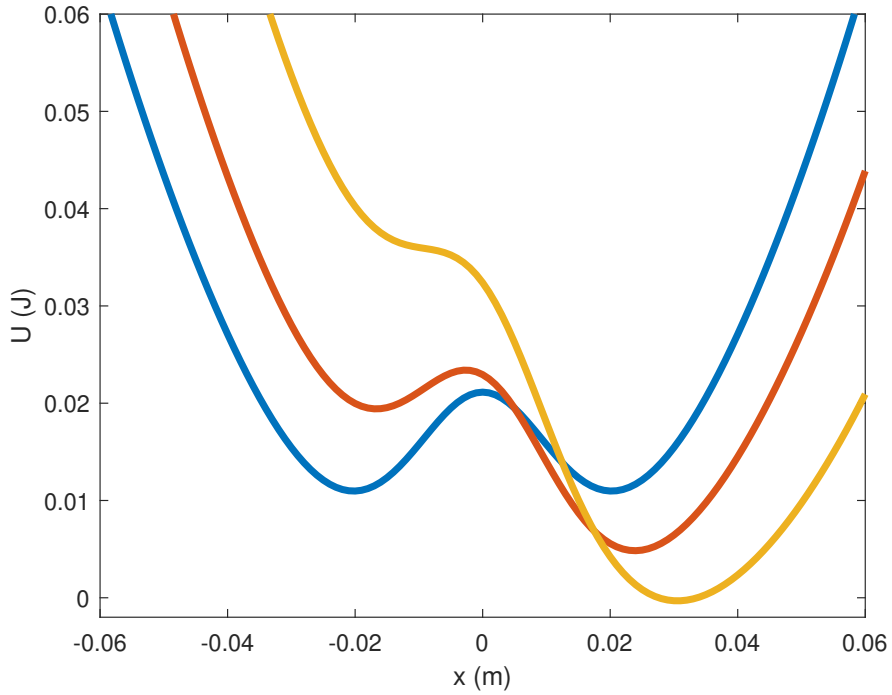

Fig. 2: U is the sum of U_b and U_m for the static fixed-free beam with (blue) fixed end w aligned at the neutral center position in line with the external magnet (red) fixed end w slightly offset in 1 direction and (yellow) fixed end w significantly offset from the center position shows only 1 stable static equilibrium when displacement is large.

$(x-w)$ is relative displacement of the beam's free end with respect to it's attachment. Collectively, the terms $3EI/L^3$ represent the spring constant k of the beam under a linear Euler-Bernoulli assumption.

Using the dipole magnetic model with magnetic potential energy calculated as the negative product of magnetization of the tip mass magnet and the magnetic field of the stationary magnet, magnetic potential energy was calculated as

$$U_m = \frac{\mu_0 M^2 V_t V_e}{4\pi}\left(\frac{(3\epsilon^2 - r^2)(\cos\theta) - 3\epsilon x \sin\theta)}{r^5}\right), \tag{6}$$

with μ_0 representing the permeability of free space, M the magnetization of each magnet (assumed that the two magnets are identical), V_t the volume of tip mass magnet, V_e the volume of the external magnet, r the separation distance, ϵ the closest distance between tip mass and external magnet along the central axis, x the displacement of the tip mass from the centerline and θ the angle of the magnetic tip mass with these dimensions as seen in Fig. (1).

Kinetic energy of the magnetic tip mass can be found using its velocity $\dot{x}$ according to

$$T = \frac{1}{2}m\dot{x}^2. \tag{7}$$

This results in a Lagrangian

$$L = T - U_s - U_m, \tag{8}$$

and the resulting equation of motion can be solved using

$$\frac{d}{dt}\left(\frac{\partial L}{\partial \dot{x}}\right) - \frac{\partial L}{\partial x} = Q \tag{9}$$

where Q represents the general forces which in this case is the assumed damping forces due to friction and any electrical harvesting components. The partial derivative of the magnetic potential is the more complicated step and its result is

$$\frac{\partial U_m}{\partial t} = f(x) = \frac{\mu_0 M^2 V_t V_e}{4\pi}\left(3\epsilon^2 C_1 - 3\epsilon C_2 - C_3\right) \tag{10}$$

where

$$C_1 = -\left(\frac{5x}{r^7}\right)\cos\theta - \left(\frac{3}{2Lr^5}\right)\sin\theta \tag{11}$$

$$C_2 = \left(\frac{3x}{2Lr^5}\right)\cos\theta - \left(\frac{5x^2}{r^7} + \frac{1}{r^5}\right)\sin\theta. \tag{12}$$

$$C_3 = -\left(\frac{3x}{r^5}\right)\cos\theta - \left(\frac{3}{2Lr^3}\right)\sin\theta \tag{13}$$

The resulting equation of motion takes the form

$$m\ddot{x} - d\dot{x} + kx + f(x) = kw\sin\Omega t \tag{14}$$

where k is the Euler-Bernoulli spring constant described above with Eq. 5, and $f(x)$ represents the nonlinear forces resulting from the magnetic interactions.

Simulated Results

Since the physical properties of the beam and magnets are difficult to adjust in a deployed setting, the same set of physical dimensions was used all of the following simulations. Experimental tuning would be conducted by altering ϵ_0, and in frequency ranges with multiple stable periodic solutions, different behaviors can be found by altering the initial conditions of the system x_i and $\dot{x}_i$. Dimensions used for these simulations are listed in Table 1.

Simulations provide the expected behavior of the system, and four different categories of stable periodic behavior have been observed. Figure 3a shows the typical low frequency, low amplitude behavior

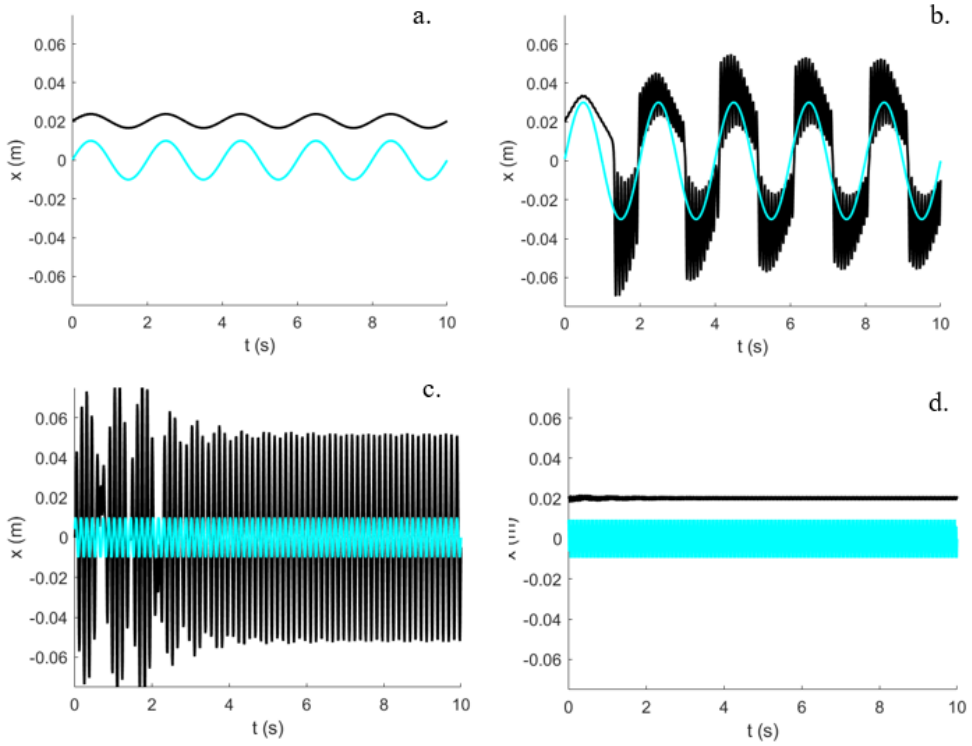

Fig. 3: The blue line represents beam's fixed end position and the black line is the position, x, of the beam's free end. The four observed system response behaviors are (a) low amplitude, low frequency intrawell periodic oscillations with excitation A = 0.01 m, ω = 0.5 Hz, (b) frequency up-conversion with excitation A = 0.03 m, ω = 0.5 Hz, (c) high amplitude interwell periodic oscillations with excitation A = 0.01 m, ω = 7.0 Hz, (d) near stationary with excitation A = 0.01 m, ω = 30.0 Hz. Units for t are seconds, and x and w are measured in meters.

where the beam's tip mass is stuck in intrawell oscillations at the excitation frequency. This is very low energy output and undesireable behavior. Figure 3b demonstrates behavior at the same low frequency as Fig. 3a but with larger amplitude. In this case, frequency up-conversion is observed when the tip mass snaps through the center magnet resulting in a significant improvement in system kinetic energy, which would result in improved energy harvested.

Near the beam's natural frequency, Fig. 3c shows that stable interwell oscillations are possible. This case will result in the largest possible harvested energy, though it may require specific initial condition to achieve this case in practice, as opposed to the frequency up-conversion case which is very easy to obtain for broad ranges of initial conditions and frequency and amplitude ranges. In this example, interwell behavior was found by altering the initial position to $x_i = 0.0$, which adds enough extra initial energy to the system to find this higher energy solution instead of a lower energy solution present when starting from static equilibrium.

Lastly, Fig. 3d shows a high frequency case in which the tip mass seems to hardly move at all. It should be noted that though the tip mass doesn't move, there is still relative motion between the fixed and free ends, so energy can be produced in this case. However, because high frequency oscillations are only physically achievable with very low amplitudes, the amount of energy generated in this case would likely be very small. This high frequency case will not be a focus of analysis in this study since the system construction does not provide any advantages over previously published models for this case, so for environments with high frequency excitation significantly above the system's natural frequency,

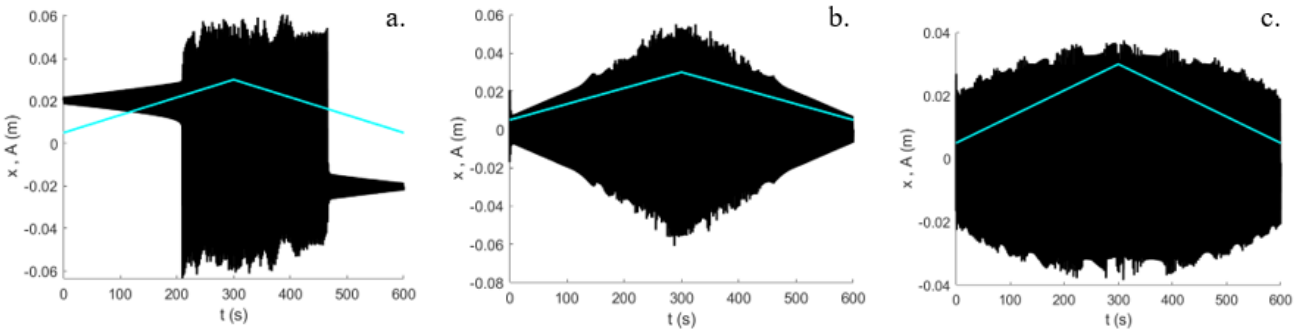

Fig. 4: The blue line represents the beam's fixed end excitation amplitude, A, which conducts a sweep up and down, and the black line is position of the beam's free end, x. Gap distance between free end and external magnets are solved using (a) B=0 (stationary), (b) B = 1 using ϵ according to Eq. 3 (c) B = 1 using ϵ according to Eq. 4

other models should be used.

The vastly different behaviors in Fig. 3a and Fig. 3b based on excitation amplitude can be problematic in environments with time varying excitation as shown in the amplitude sweep of Fig. 4a where the first 200 seconds show low amplitude, low frequency intrawell vibration before an excitation amplitude threshold is reached, after which frequency up-conversion happens as the magnet snaps through the external magnet each cycle. In order to achieve the higher energy, frequency up-conversion behavior at all oscillation amplitudes, the separation distance ϵ needs to be reconfigured to be a larger gap at lower amplitudes, lowering the potential well escape threshold. However, active tuning is undesireable in energy harvesting devices. These devices only harvest low amounts of energy, and any active tuning control system is likely to use up the small amounts harvested. Thus any tuning system must operate passively. Simulated results for two construction techniques are provided. Figure 4b demonstrates simulated results of a construction that follows Eq. 3 with ϵ as a function of the excitation amplitude. With a fixed value of ϵ, low amplitude oscillations are stuck in low-energy intrawell behavior. However, by varying ϵ it is possible to achieve the higher energy snap-through behavior even at low amplitudes.

Figure 4c shows simulated results using Eq. 4 so that the separation distance oscillates closer/further from the tip mass in phase with the fixed end excitation so that the magnet is pulled closest to the beam when the excitation is largest from centerline, and the magnet is pushed furthest away from the beam when the excitation is at the system centerline. This last case provides the same frequency up-conversion as in Fig. 3b, but has the effect of flattening the response curve with much higher amplitude vibrations at low excitation levels, but much lower amplitude vibrations at the highest excitation levels.

As a simplification, instead of modeling an electric circuit, relative kinetic energy of the tip mass will be used as a correlated value, where it is expected that a higher relative kinetic energy of the tip mass is expected to harvest greater energy by its associated piezoelectric device. Relative kinetic energy (with respect to the fixed end) is more relevant than its absolute kinetic energy since no changes in strain energy are induced in the beam when the fixed and free ends are moving in sync with each other. It is only their differences in motion that cause bending and therefore create strain energy to be harvested. T_e will be used to represent this correlated measure with the equation

$$T_e = \frac{1}{2} m(\dot{x} - \dot{w})^2. \tag{15}$$

In a previous cantilever beam energy harvester [12], the external magnet was fixed to the external

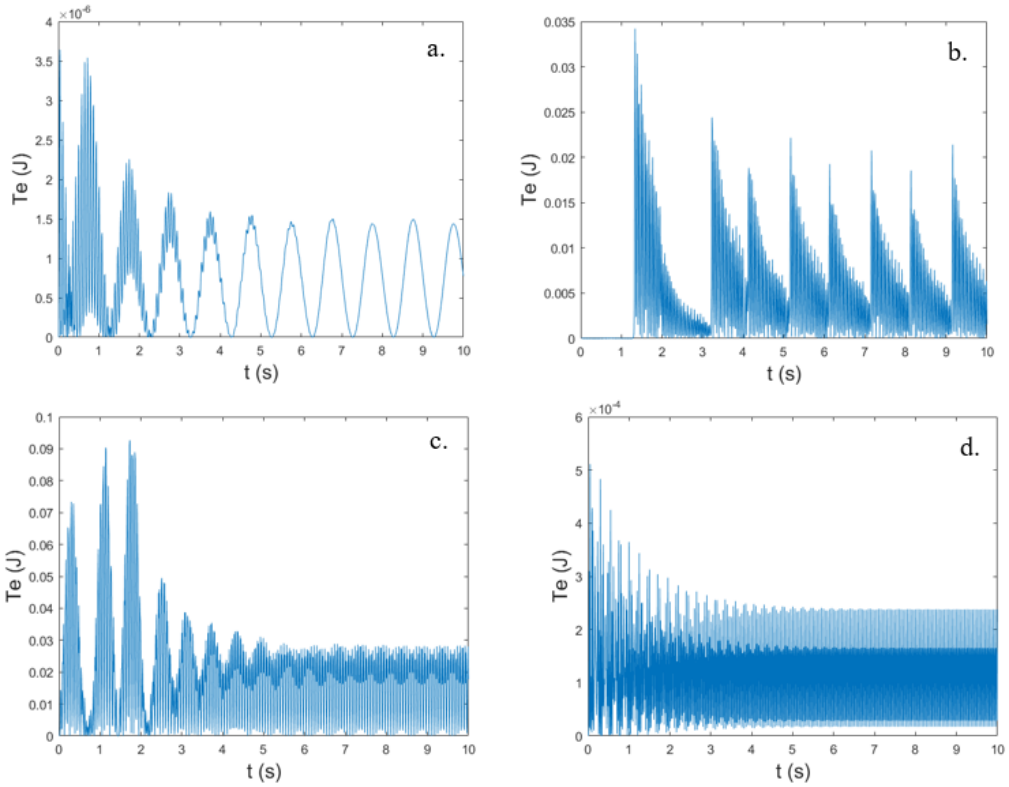

Fig. 5: The four subplots (a)-(d) match the same conditions as Fig. 3a-d but instead of position, show the relative kinetic energy of the tip mass when subjected to each form of excitation.

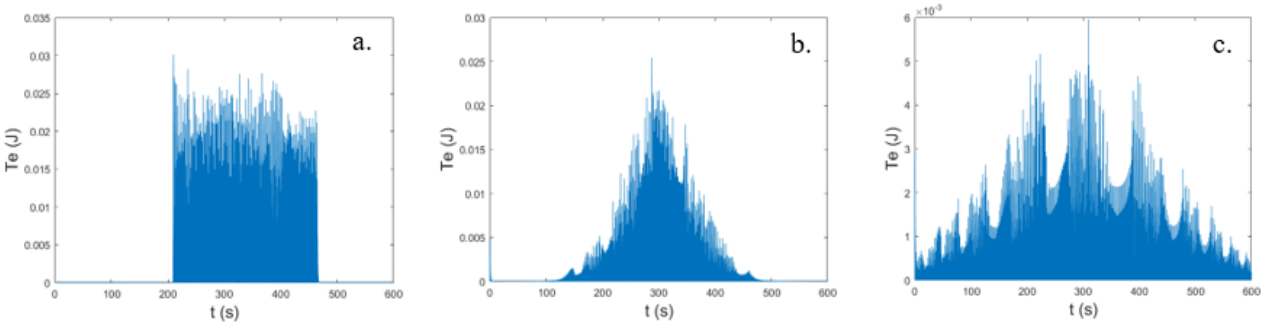

Fig. 6: The three subplots (a)-(c) match the same conditions as Fig. 4a-c but instead of position, show the relative kinetic energy of the tip mass when subjected to each form of excitation.

excitation and moved along with the beam's fixed end. This resulted in a constant potential energy curve that was always bistable at all points in time. However, the downside to that system was system results were very dependent on initial conditions due to the present of coexisting solutions near the natural frequency, and only very low energy solutions were possible at frequencies much lower than the natural frequency. In these cases, the low amplitude intra-well solution is usually the easiest to obtain, but the less desirable. Qualitatively, that low energy intrawell behavior is similar to that observed in Fig. 3a. Figures 5a-b clearly demonstrate the advantage of the stationary external magnet over the case of external magnet oscillating in line with the fixed end by showing the multiple order of magnitude

increase in kinetic energy of the frequency up-converted case of Fig. 5b over the relative energy in the low-frequency intrawell oscillations of Fig. 5a. As expected, the high-frequency, interwell oscillations in Fig. 5c result in the largest relative kinetic energy, and the nearly stationary tip mass subjected to very high frequency oscillations results in a relatively lower relative kinetic energy as seen in Fig. 5d.

Figure 6 shows relative kinetic energy for the three ϵ equations used for Figure 4. Readers should note that the y-axis scale for Fig. 6c is different than the other two subplots. Although Fig. 6b provides energy over a wider amplitude range than Fig. 6a, this can come at a significant expense of energy, though it is suspected that this may be overcome through tuning of ϵ_0 and B in the separation distance function for ϵ. Figure 6c shows the widest energy range of the three cases, but its peak is much lower, again suggesting that improved tuning may be required to optimize the system's performance.

Conclusion

This paper investigated a piezoelectric energy harvester by modeling the expected behavior of a bistable cantilever beam system with magnetic tip mass and external tip mass in order to demonstrate how various manipulations of the separation distance can provide a more efficient harvester than previously investigated. The main problem similar systems face is low energy harvested when subjected to excitation frequencies significantly below the system's natural frequency. This harvester allows frequency up-conversion at low frequency ranges as long as sufficient excitation amplitude is available. Two mathematical models for altering the strength of the bistability of the system were provided as proposed solutions to the case where only low amplitude excitation is available.

While this paper showed some qualitative benefits to varying the separation distance, simultaneous quantitative benefits in peak power and amplitide robustness have not yet been realized. The parameters for this study allowed the ability to demonstrate expected behavior types, which can prove useful for determining ranges for parameters prior to experimentation rather than during. Future work for this system would require analytical tuning to determine optimal functions for ϵ. A physical experiment would also positively contribute to the field by demonstrating the construction methods for passively reconfiguring the separation distance ϵ, and supporting the validity of these mathematical models and simulated results.

Acknowledgements

This research was supported by Human Frontiers of Science Program Grant RPG 24/2012 and the National Science Foundation DMS-1412119, and Department of Education, Title 3, HSI-STEM, Award : P031C160145.

References

References

[1] Anton, S. R., and Sodano, H. A., 2007. "A review of power harvesting using piezoelectric materials (2003–2006)". *Smart Materials and Structures,* **16**(R1).

[2] Erturk, A., and Inman, D. J., 2009. "An experimentally validated bimorph cantilever model for piezoelectric energy harvesting from base excitations". *Smart Materials and Structures,* **18**, p. 025009.

[3] Beeby, S. P., Tudor, M. J., and White, N. M., 2006. "Energy harvesting vibration sources for microsystems applications". *Measurement Science and Technology,* **17**(12), Oct., pp. R175–R195.

[4] Liu, J.-Q., Fang, H.-B., Xu, Z.-Y., Mao, X.-H., Shen, X.-C., Chen, D., Liao, H., and Cai, B.-C., 2008. "A mems-based piezoelectric power generator array for vibration energy harvesting". *Microelectronics Journal,* **39**, pp. 802–806.

[5] Meruane, V., and Pichara, K., 2015. "A broadband vibration-based energy harvester using an array of piezoelectric beams connected by springs". *Shock and Vibration,* **2016**(9614842), August, pp. 1–13.

[6] Challa, V. R., Prasad, M. G., and Fisher, F. T., 2008. "High efficiency energy harvesting device with magnetic coupling for resonance frequency tuning". In Proc. SPIE, M. Tomizuka, ed., Vol. 6932, pp. 1–12.

[7] Bernard, B. P., and Mann, B. P., 2018. "Increasing viability of nonlinear energy harvesters by adding an excited dynamic magnifier". *Journal of Intelligent Systems and Structures,* **29**(6), pp. 1–10.

[8] Van Blarigan, L., Danzl, P., and Moehlis, J., 2012. "A broadband vibrational energy harvester". *Applied Physics Letters,* **100**, p. 253904.

[9] Friswell, M. I., Ali, S. F., Bilgen, O., Adhikari, S., Lees, A. W., and Litak, G., 2012. "Non-linear piezoelectric vibration energy harvesting from a vertical cantilever beam with tip mass". *Journal of Intelligent Material Systems and Structures,* **23**(13), pp. 1505–1521.

[10] Vocca, H., Neri, I., Travasso, F., and Gammaitoni, L., 2012. "Kinetic energy harvesting with bistable oscillators". *Applied Energy,* **97**, pp. 771–776.

[11] Harne, R. L., and Wang, K. W., 2013. "A review of the recent research on vibration energy harvesting via bistable systems". *Smart Materials and Structures,* **22**(12), p. 023001.

[12] Stanton, S. C., MgGehee, C. C., and Mann, B. P., 2010. "Nonlinear dynamics for broadband energy harvesting: Investigation of a bistable piezoelectric inertial generator". *Physica D,* **239**, pp. 640–653.

[13] Wang, F., Abedini, A., Alghamdi, T., and Onsorynezhad, S., 2019. "Bimodal approach of a frequency-up-conversion piezoelectric energy harvester". *International Journal of Structural Stability and Dynamics,* **19**(08).

[14] Abedini, A., Onsorynezhad, S., and Wang, F., 2019. "Periodic solutions of an impact-driven frequency up-conversion piezoelectric harvester". *International Journal of Bifurcation and Chaos,* **29**(10).

[15] Feeny, B. F., and Diaz, A. R., 2010. "Twinkling phenomena in snap-through oscillators". *Journal of Vibration and Acoustics,* **132**(7), December, p. 061013.

[16] Panigrahi, S. R., Bernard, B. P., Feeny, B. F., Mann, B. P., and Diaz, A. R., 2017. "Snap-through twinkling energy generation through frequency up-conversion". *Journal of Sound and Vibration,* **399**, March, pp. 216–227.

[17] Pozzi, M., and Zhu, M., 2011. "Plucked piezoelectric bimorphs for knee-joint energy harvesting: modelling and experimental validation". *Smart Materials and Structures,* **20**(5), p. 055007.

[18] Zhu, W. Z., and Livermore, C., 2015. "Passively-switched, non-contact energy harvester for broad operational range and enhanced durability". *Journal of Physics: Conference Series,* **660**, dec, p. 012119.

[19] Edwards, B., Aw, K. C., and Hu, A. P., 2016. "Mechanical frequency up-conversion for sub-

resonance, low-frequency vibration harvesting". *Journal of Intelligent Material Systems and Structures,* **27**(16).